6. Oscillatory Stability and RE Design

In chapter 4 and 5, it was clarified that voltage stability and transient synchronous stability are deeply influenced by power system model (power system load model and aggregation method) and design of highly penetrated RE (drop, FRT, and DVS type). In the chapter, it will be clarified how oscillatory stability that appears as power-swing with around 2 sec period is influenced by system modeling and RE design.

History of Oscillatory Stability Study

Power swing seems to occur more often than voltage collapse and asynchronism. The author has experienced twice. The first occurred in 1981. Around 2 sec period power swing lasted and it was reported that signal at busy quarter repeated on and off. Recording equipments in those days were so poor that there are no data to be introduced. By the opportunity, the author was converted from power distribution section to more academic power system section. The problem to be solved first was that the newly introduced simulation tool could not represent the power swing phenomenon. By investigation it became clear that data were not correct. By gathering, ordering, and applying minute data of generators, excitation systems, and speed governing systems, power swing was represented, but a little severer than reality. As a temporary countermeasure, 1 p.u. virtual damping was applied on generator shafts was employed and simulation became agree well to the reality. Later, hearing from a peer engineer said that load's frequency character had damping effect on power swing, 2 p.u. load's frequency sensitivity was employed instead of the former 1 p.u. virtual damping. The result was quite well. Power swing occurs in some generators and infinite bus. Load locates almost midway from generator to infinite bus. Therefore, frequency deviation at load is almost half of generator speed deviation. Thus, 2 p.u. load's frequency sensitivity has the same effect as 1 p.u. virtual damping at generator shaft.
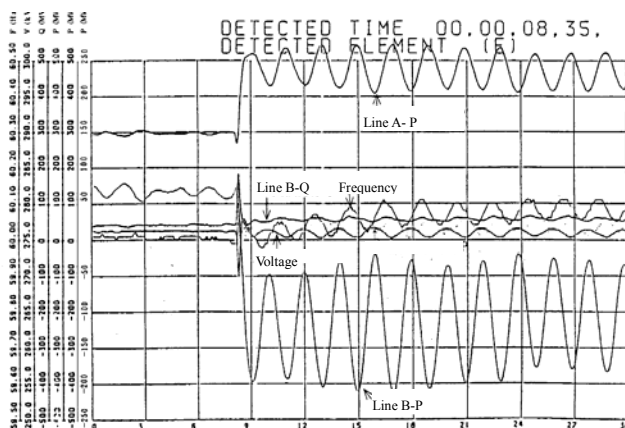

Fig. 6.1 power swing in 1985

The second occurred in 1985. 2 sec period power swing appeared again. In those days good measuring equipments are already employed and data such as Fig. 6.1 were recorded. To say the truth, the author predicted the phenomenon. Terminal voltage record of thermal generator's load reject test is represented further better by assuming quadrature axis transient components (Xq' and Tq') than ignoring them. By assuming those components, calculated maximum tie line operational power flow was reduced to 200MW

(sending) from those day's standard, 400MW. Margin was negative! Of course the author warned. But boss ignored the warning. Soon, the power swing appeared at 180MW tie line power flow. The warning was verified. Boss of the boss became very angry and said "Son of a bitch!" Soon PSS (Power System Stabilizer) were equipped on thermal generators. After the incident in the utility employing the author, quadrature axis transient components are considered. However in most other utilities, those components seem ignored.

By the way, the reason why the author focused in representation of exciting system at 1982 when the author was converted is history and fruits on oscillatory stability research. The first is Ref. (1) by Heffron and Philips. The contents were introduced in Ref. (2), which the author studied. However, these focused in rather extending leading power factor operation of synchronous generator. It was Ref. (3) by Demmelo and Concordia in 1969 that focused in relation between power swing and excitation system design. However, these three ancestors employed "one machine infinite bus model" and load neighboring the generator was ignored. The model is realistic in the case that large remote power source sends much power to power pool, but is not realistic in the case that a large interconnection is divided in two parts and power swing appears among the two parts. In addition, influence of load modeling, aggregation, and RE cannot be dealt. Ref. (4) and (5) by Komami and Komukai in 1987 extended Demmelo-Concordia theory and consider midway load having voltage sensitivity. Ref. (6) by Yamagishi and Komami analyzed oscillatory stability with highly penetrated RE (Renewable Energy). Since contents of the chapter are mainly based on Komami-Komukai theory, it is introduced first. Fundamental equations of synchronous generator for solving oscillatory stability elegantly are Ref. (7) by Kimbark and the book wad republished, but perhaps only very few engineers have read it. At last a block diagram is conducted. But a paper cannot explain the process by limitation of volume, and therefore, only makes citation. As time goes by, a world that no one knows truth. To avoid such a situation, the author intends to record the whole process in the chapter.

Komami-Komukai Theory

One machine and infinite bus model with midway load is the minimum model for oscillatory stability analysis. The structure is shown in Fig. 6.2. All network paths from trunk system to load terminal are considered.
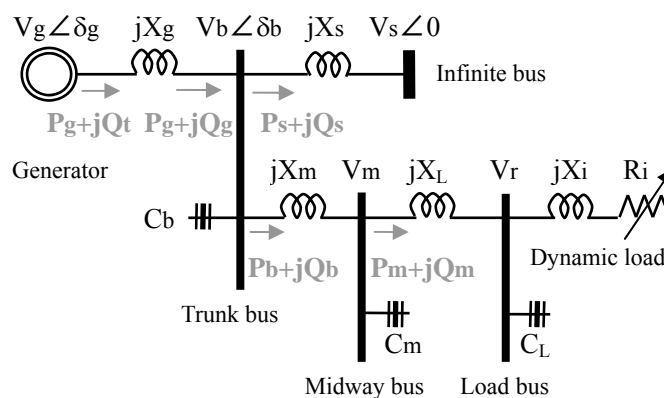

Fig. 6.2 Minimum model for oscillatory stability analysis

Oscillatory stability analysis deals with small variation around the operating point. Voltage sensitivity of load seen from trunk bus affects character of the whole system. By IM's dynamic character, the sensitivity is different in steady state and transient. The theory considers the sensitivity as parameter.

Conducting fundamental equations of synchronous generator are minutely written in Ref. (7). Here, the results are listed up as follows.

$$\mathbf{Vt} = Vd + j\, Vq \qquad \mathbf{I} = Id + j\, Iq \qquad \mathbf{\Psi} = \Psi d + j\, \Psi q$$

$$Vd = s\, \Psi d - \Psi q\, s\, \theta \qquad\qquad Vq = s\, \Psi q + \Psi q\, s\, \theta$$

$$\Psi d = If - Xd\, Id \qquad\qquad \Psi q = -\, Xq\, Iq \qquad\qquad (6.1)$$

$$\Psi fd = If - (Xd - Xd')\, Id \qquad Efd = If + Tdo'\, s\, \Psi fd$$

$$\frac{M\, s\, \delta}{\omega_0} = Tm - Te \qquad\qquad Te = \Psi d\, Iq - \Psi q\, Id + \frac{D\, s\, \delta}{\omega 0}$$

Symbols used here are explained. However, the meanings and that of equation (6.1) must be not clear for beginners. The meaning will be understood by long research life. For the instance, it is sufficient to understand what can be understood.

Vt : terminal voltage,   Vd : its direct axis component,   Vq : its quadrature axis component,

I : current,   Id : its direct axis component,   Iq : its quadrature axis component,

Ψ : flux linkage of armature winding, Ψd : its direct axis component,

Ψq : its quadrature axis component,   s : Laplace transform, θ : rotor position

If : field current, Ψfd : flux linkage of field winding,

Xd : direct axis synchronous reactance,   Xq : quadrature axis synchronous reactance,

Xd' : direct axis transient reactance,   Efd : field voltage,

Tdo' :   : direct axis open circuit transient time constant,

M : unit inertia constant (sec), δ : rotor phase angle, ω_0 : system frequency,

Tm : mechanical input torque,   Te : electric output torque,   D :   : damping coefficient

Power flow conditions are expressed as follows.

$$Pg = \frac{Vt\, Vb\, \sin(\delta t - \delta b)}{Xt} \qquad\qquad Qg = \frac{Vt\, Vb\, \cos(\delta t - \delta b) - Vb^2}{Xt}$$

$$Ps = \frac{Vb\, Vs\, \sin \delta b}{Xs} \qquad\qquad Qs = \frac{Vb^2 - Vb\, Vs\, \cos \delta b}{Xs} \qquad\qquad (6.2)$$

Small variations of load are expressed as follows by using voltage sensitivities α, β, and γ. Here, Qc is reactive power supplied by trunk bus capacitor Cb, and calculated as $Qc = Cb\, Vb^2$.

$$\varDelta Pb = \alpha\, Pb\, \frac{\varDelta Vb}{Vb} \qquad\qquad \varDelta Qb = \beta\, Qb\, \frac{\varDelta Vb}{Vb} \qquad\qquad \varDelta Qc = \gamma\, Qc\, \frac{\varDelta Vb}{Vb} \qquad (6.3)$$

As to small variation of active and reactive power, two equations as follows are conducted.

$$\Delta Pg = \Delta Pb + \Delta Ps \qquad \Delta Qg = \Delta Qb + \Delta Qs - \Delta Qc \qquad (6.4)$$

By power flow condition (6.2), four small variations: ΔPg, ΔQg, ΔPs, and ΔQs can be expressed by the other four small variations: ΔVt, ΔVb, $\Delta \delta t$, and $\Delta \delta b$. Substituting the relations between those 8 small variations and equation (6.3) to (6.4), two equations consists of only four small variation: ΔVt, ΔVb, $\Delta \delta t$, and $\Delta \delta b$. Equations conducted above are applied to fundamental equations of synchronous generator, and omitting minute process, finally equations as follows are conducted.

$$\Delta Pg = K_1 \, \Delta \delta + K_2 \, \Delta Vt$$

$$T_{do}' \, s \, \Delta \Psi fd = \Delta Efd - K_3 \, \Delta \Psi fd - K_4 \, \Delta \delta \qquad (6.5)$$

$$\Delta Vt = K_5 \, \Delta \delta + K_6 \, \Delta \Psi fd$$

These three equations can be integrated and expressed as a block diagram as shown Fig. 6.3. It must be noticed that here conducted block diagram has the same form of that ignoring midway load in Ref. (3), excepting change in coefficients K_1 to K_6 by load. These six coefficients are real numbers decided by only operating condition, and never vary the other factor such as power swing period. The block diagram is sometimes called as "Demello's diagram", and the coefficients are called as "Demello's coefficients". The paper in 1969 persuades that excessively high gain excitation system spoils oscillatory stability, and made elegant analysis of oscillatory stability possible. The author highly evaluates but physics and mathematics used are so difficult that most engineers keep respectable distance, and penetration seems not wide.
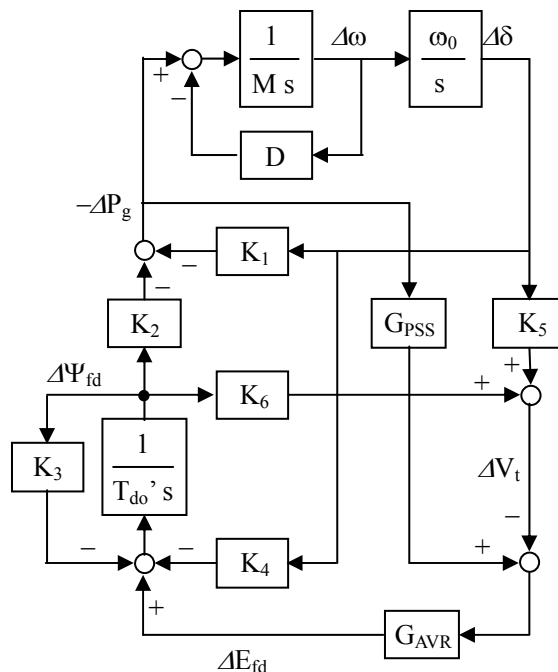

Fig. 6.3 Demello's block diagram

Paths from $\Delta \delta$ to ΔPg can be integrated and expressed as follows.

$$\Delta Pg = \frac{K_1 \, (K_3 + T_{do}' \, s + K_6 \, G_{AVR}) - K_2 \, K_4 - K_2 \, K_5 \, G_{AVR}}{(K_3 + T_{do}' \, s + K_6 \, G_{AVR}) + K_2 \, G_{AVR} \, G_{PSS}} \, \Delta \delta = (Ks + jKd) \, \Delta \delta \qquad (6.6)$$
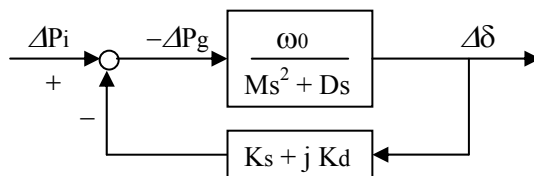

Fig. 6.4   Simplified block diagram

Using the equation (6.6), Demello's block diagram can be equivalently transformed as shown in Fig. 6.4. Here, K_s and K_d are quantities varying by swing period. K_s is called as "synchronizing torque coefficient", and K_d is called as "damping torque coefficient".

Voltage sensitivity of dynamic load such as IM is different in steady state and transient. Rotating speed of IM does not vary by slight contingency because of inertia. Therefore, IM internal resistance also does not vary, and in transient condition IM can be expressed as constant impedance. As time goes by, IM speed and resistance vary so as to fulfill mechanical power demand without considering system condition. Thus, IM turns to constant power load.

As a method to integrate the transient and steady states, Demello's coefficients K_i' (I = 1 to 6) calculated by regarding IM as constant impedance load and those K_{i0} (i = 1 to 6) calculated by regarding IM as constant power load are integrated to extended Demello's coefficients K_i' (i = 1 to 6) as follows.

$$K_i(s) = \frac{K_{i0} + K_i' \, T \, s}{1 + T \, s} \qquad \text{for i=1,6} \qquad (6.7)$$

K_i is no longer a real number but a complex number that varies by swing period. However, Demello's block diagram is still valid. Time constant T is, by measured data, around 0.05 sec or so.

Voltage Sensitivity of Load

In analyses hereafter, sensitivity of load reactive power β sometimes becomes negative. Many engineers show a kind of rejection against it. Therefore, at first, the author intends to verify that voltage sensitivity of existing load's reactive power can be negative. Measured data of active and reactive power by voltage on existing pump-motor load are shown in Fig. 6.5. Vertical and horizontal axes are expressed in logarithm graduation. Active power in loaded condition P is almost constant by voltage. The tendency, constant power is one of IM load characters.
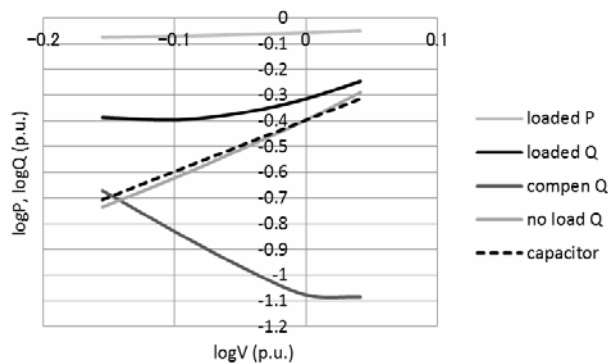

Fig. 6.5   Voltage sensitivity of IM compensated by capacitor

Behavior of load's reactive power Q is not constant. In no load condition, Q is almost proportional to square voltage, that is, constant impedance. IM is usually equipped with capacitor that compensates no load reactive power of IM approximately. Since the capacitor is also constant impedance, the compensation is effective at any voltage. When compensated, IM reactive power in loaded condition calculated from measured data is proportional to -2 or -3 times powered voltage. Since it must be theoretically proportional to -2 times powered voltage, the value -2 is used hereafter.

Load's voltage sensitivities seen from trunk bus and midway bus must be different from those at load bus. The difference are derived from series reactance and shunt capacitor in network. At first, how voltage sensitivity varies by series reactance is calculated. Structure of minimum model is shown in Fig. 6.6.
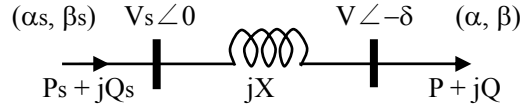

Fig. 6.6 Load fed via series reactance

Voltage sensitivities of load itself are assumed as α in active power and β in reactive power. Voltage sensitivities seen via series reactance X are assumed as αs in active power and βs in reactive power. Those assumptions are expresses as follows.

$$\alpha s = \frac{\Delta Ps / Ps}{\Delta Vs / Vs} \qquad \beta s = \frac{\Delta Qs / Qs}{\Delta Vs / Vs} \qquad \alpha = \frac{\Delta P / P}{\Delta V / V} \qquad \beta = \frac{\Delta Q / Q}{\Delta V / V} \qquad (6.8)$$

Power flow conditions are expressed as follows.

$$P = \frac{Vs\, V \sin \delta}{X} \qquad Q = \frac{Vs\, V \cos \delta - V^2}{X}$$

Erasing phase angle δ, relation as follows is obtained.

$$Vs^2 = V^2 + 2XQ + \frac{X^2}{V^2}\,(P^2 + Q^2) \qquad (6.9)$$

Taking small variation of equation (6.9), and applying equation (6.8) to it, relation as follows is obtained.

$$Vs^2\, \frac{\Delta Vs / Vs}{\Delta V / V} = V^2 + XQ\beta + \frac{X^2\, P^2}{V^2}\,(\alpha - 1) + \frac{X^2\, Q^2}{V^2}\,(\beta - 1) \qquad (6.10)$$

Here, voltage variation rate ratio at both sides κ can be calculated as follows.

$$\kappa = \frac{\Delta Vs / Vs}{\Delta V / V} = \frac{V^2 + XQ\beta}{Vs^2} + \frac{X^2}{Vs^2\, V^2}\,\{\, P^2\,(\alpha - 1) + Q^2\,(\beta - 1)\,\} \qquad (6.11)$$

Active power does not varies if seen via reactance, that is, $Ps = P$, $\Delta Ps = \Delta P$. Therefore,

$$\alpha s = \frac{\Delta Ps / Ps}{\Delta Vs / Vs} = \frac{\Delta P / P}{\Delta V / V}\, \frac{\Delta V / V}{\Delta Vs / Vs} = \frac{\alpha}{\kappa} \qquad (6.12)$$

Reactive power increases if seen via reactance due to reactive power loss as follows.

$$Qs = Q + \frac{X\,(P^2 + Q^2)}{V^2}$$

Taking small variation, relations as follows are obtained.

$$Q_s \frac{\Delta Q_s}{Q_s} = Q \frac{\Delta Q}{Q} + \frac{2XP^2}{V^2}\left(\frac{\Delta P}{P} - \frac{\Delta V}{V}\right) + \frac{2XQ^2}{V^2}\left(\frac{\Delta Q}{Q} - \frac{\Delta V}{V}\right)$$

$$\kappa Q_s \beta_s = Q \beta + \frac{2XP^2}{V^2}(\alpha - 1) + \frac{2XQ^2}{V^2}(\beta - 1)$$

$$\beta_s = \frac{Q \beta}{\kappa Q_s} + \frac{2X}{\kappa Q_s V^2}\{P^2(\alpha - 1) + Q^2(\beta - 1)\} \qquad (6.13)$$

Thus, load's voltage sensitivities seen via reactance X, α_s and β_s are obtained.

Existing power system load can be assumed as mixture of IM and CZ (constant impedance). Voltage sensitivities of entire load will vary by IM ratio. In addition, influence of structure introduced in Fig. 6.2. Therefore, voltage sensitivities seen from trunk system must be much different from those of load itself, and calculation results are introduced in power sending system and receiving system.

In Table 6.1, constants of power sending system are shown.

Table 6.1   Load constants in power sending system (load power base, send)

Xm	Xr	Xi	Vb	Vm	Vr
0.246459	0.184815	0.1	1.0	1.0	0.960171

Pb + jQb	Pm + jQm	jQmc	Pr + jQr
1.0+j0.125160	1.0+j0.312656	j0.437816	1.0+j0.109775

Calculated load's voltage sensitivities of sending system at load bus (α_r and β_r), seen from midway bus (α_m and β_m), and seen from trunk bus (α_s and β_s) are shown in Fig. 6.7. It must be noticed that voltage sensitivity of reactive power seen from trunk bus β_s shows very large negative value because of much amount of capacitor (around 40% of load) at midway bus.
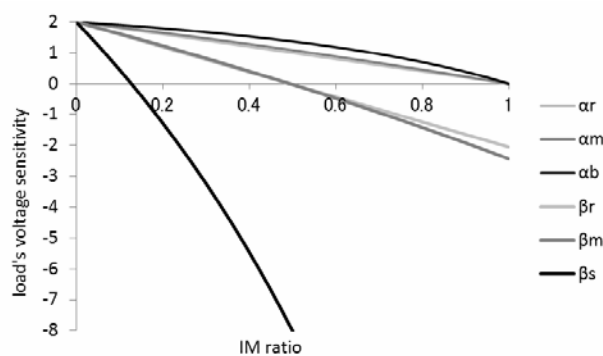

Fig. 6.7   Voltage sensitivity by observation bus (send)

Table 6.2   Load constants in power sending system (load power base, receive)

Xm	Xr	Xi	Vb	Vm	Vr
0.290402	0.155867	0.1	1.0	1.0	0.952890

Pb + jQb	Pm + jQm	jQmc	Pr + jQr
1.0+j0.184401	1.0+j0.281792	j0.397668	1.0+j0.110132

Similarly calculations are performed in power receiving system. Load constants are shown in Table. 6.2. Calculation results are shown in Fig. 6.8. Here also voltage sensitivity of reactive power seen from trunk bus βs shows very large negative value.
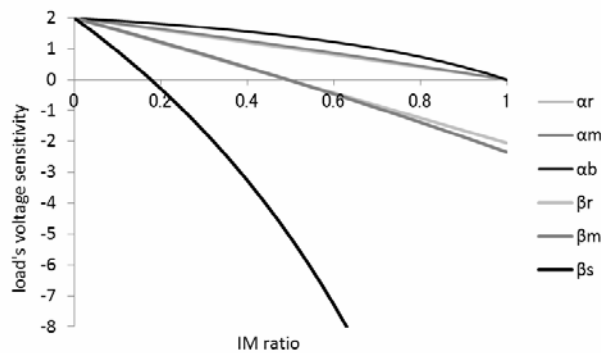

Fig. 6.7   Voltage sensitivity by observation bus (receive)

It is natural that calculated results are almost same in power sending system and receiving system. Because, difference of sending and receiving is derived from only generated power amount, and no reasons exist that indicate difference in route from trunk bus to load terminal. That is recognized by the fact that load constants are not much different in power sending and receiving systems.

Much amount of RE affects voltage sensitivities. RE is assumed to penetrate by 20% of load. Because of demand supply balance, some thermal generators are stopped. In oscillatory stability, small contingency is given in simulation. Therefore, RE and load do not stop partially, because voltage sag does not appear, and drop type RE and FRT type RE show the same behavior. RE is expressed as negative load, and its voltage sensitivities are assumed as follows. Here, W_{RE} is rated capacity of RE.

$$P_{RE} = P_{RE0} (V_{RE} /V_{RE0})^{A} \qquad Q_{RE} = W_{RE} \{ (V_{RE} / V_{RE0})^{2} - (V_{RE} /V_{RE0})^{B} \} \qquad (6.14)$$

Since RE reactive power is zero, voltage sensitivity of reactive power cannot be defined at reactive power output base, but can be defines at active power base as $2 - B$. B is 2 in case of drop and FRT types, and is assumed as 12 in case of DVS type. Voltage sensitivities of RE and load mixture are expressed as follows.

$$\alpha_{L}{}' = \frac{\alpha_{L} P_{L} - A P_{RE}}{P_{L} - P_{RE}} \qquad \beta_{L}{}' = \frac{\beta_{L} Q_{L} - (2 - B) W_{RE}}{Q_{L}} \qquad (6.15)$$

Here, α_{L} and β_{L} are voltage sensitivities of active and reactive power of load itself, $\alpha_{L}{}'$ and $\beta_{L}{}'$ are those of mixed RE and load, P_{L} and Q_{L} are load's active and reactive power, and P_{RE} is RE's active power.

Excitation System and Power System Model

Oscillatory stability is much influenced by excitation system design. To assess the influence, excitation system is modeled as shown in Fig. 6.9, where two parameters as follows exist.

Exciter time constant T_e is assumed as 2 sec in slow system, 0.5 sec in fast system.

PSS gain G_p is assumed as 0.5 when used, as 0 when not used.

Thus, four types of excitation system are considered. Difference of slow system and fast system is shown as Bode diagram in Fig. 6.10. At typical power swing period 0.5 sec, gains are not different much, but

phase in slow system is around 30 degree delayed from that in fast system. Much phase delay must spoil stability in any feedback system. Oscillatory stability with slow excitation system must be poor.
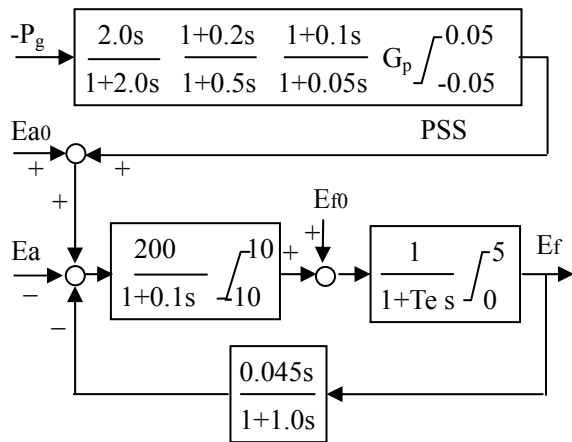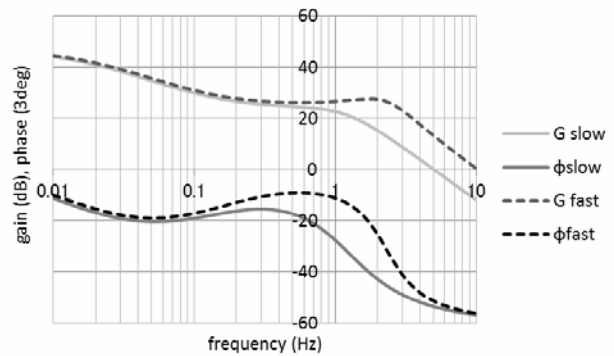

Fig. 6.9   Assumed excitation system

Fig. 6.10   Frequency response by excitation system speed

As to power system model, three kinds of load model as follows are considered.

IM : Mixture of 50% IM and 50% CZ

CI : Active power is constant current, reactive power is constant impedance. (general in Japan)

CZ : Both active and reactive power are constant impedance.

Two kinds of aggregation method are considered.

Y : Y-connection aggregation

T : Traditional aggregation

Thus, 3 by 2 equal 6 types of power system model are considered. But in case of CZ load, Y-connection and traditional method give the same results. Therefore, there are 5 power system model to be considered.

Example of Power Sending System
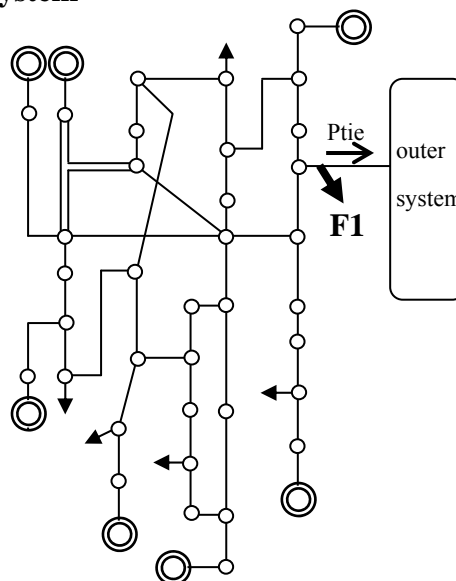
Fig. 6.11   Structure of sending system

Structure of the example power sending system is shown in Fig. 6.11. One circuit disconnection on two-circuit transmission line at F1 is assumed as small contingency. Power flow conditions after contingency are shown in Table 6.3.

Table 6.3   Power flow conditions of sending system

Xt	Xs	Vt	Vb	Vs	Pg	Pb	Ps
0.2061	4.7804	1.025	1.0	1.0	0.7601	0.6971	0.0629

[**IM Ratio**]   When IM ratio is varied, Demello's coefficients in steady state vary as Fig. 6.12. Roughly saying, positive value of the coefficient indicates stable and negative value unstable. Stability distinction is not perfect by the coefficients because of the other influences such as damper winding, but helpful.

At a glance, a singular point exists at 70% or a little more IM ratio. In higher IM ratio, K_2 goes to negative, which means that generator output reduces if excitation is increased. In such a situation, no excitation system can perform stable operation.

K_5 shows negative value even if IM ratio is zero. This is a special character of power sending system. That does not necessarily means oscillatory instability because of damping of generator itself, but at least means that oscillatory instability is more possible in power sending system.
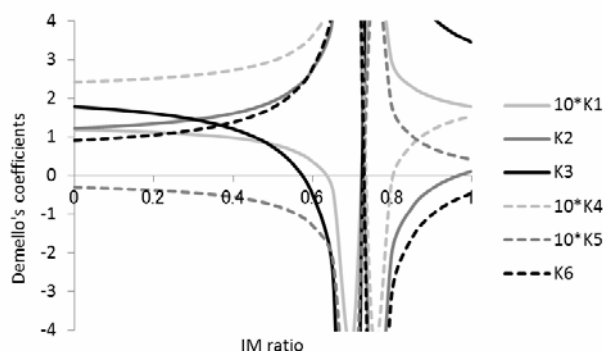

Fig. 6.12   Demello's coefficients by IM ratio (send)

As IM ratio increase, K_5 increases its negative value and falls into unstable before reaching the singular point. Next, K_3 and K_1 turn to negative. Thus, IM makes oscillatory stability worse. In sending system, instability due to negative K_5 is dominant. However, instability due to negative K_5 or K_3 can be mitigated by careful design in excitation system.

[**Excitation System**]   Four types of excitation system introduced above are compared. As system model, most realistic combination: IM 50% load and Y-connection aggregation is adopted. Damping torque coefficients are shown in Fig. 6.13. The value goes to negative at 1 Hz or slower frequency if PSS is not used. The negative value is not solved by PSS if excitation system is slow. By combination of PSS and fast excitation system, stability is improved to almost zero.

Absolute stability distinction is not possible by damping torque coefficient, but possible by Nyquist trajectory, the simplest measure, as shown in Fig. 6.14. The trajectory can be drawn by plotting open loop complex gain of the system with increasing frequency. As frequency increase plotted point goes to zero point. In the process, if point (-1, 0) is always seen at left side, the system is stable. In the figure,

combination of PSS and fast excitation system is only judged as just stable.
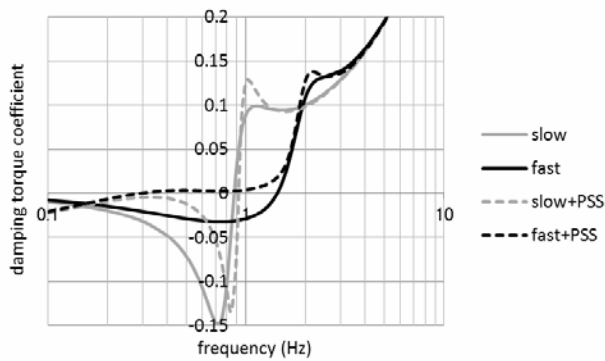

Fig. 6.13 damping torque by excitation system design (send)
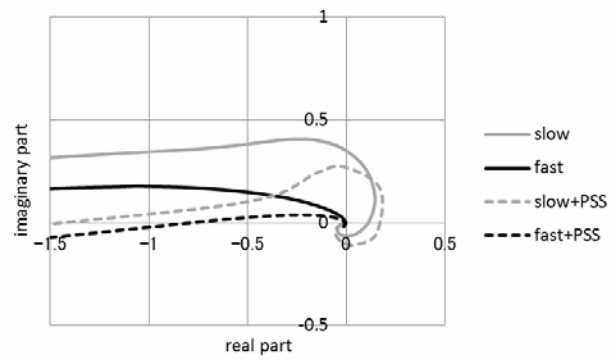

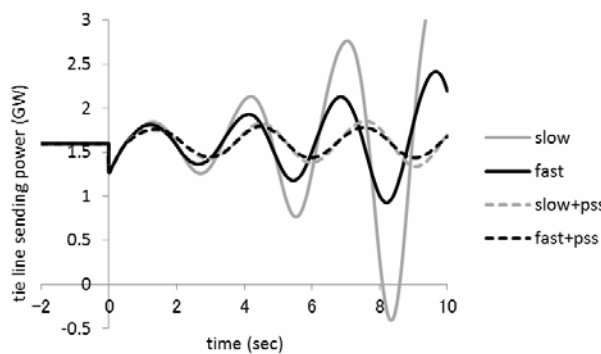Fig. 6.14 Nyquist trajectories and excitation system design (send)

Fig. 6.15   Simulation by excitation system design (send)

As the final measure, simulation is employed. The results are shown in Fig. 6.15. Combination of PSS and fast excitation system only shows stabile result. The other three cases show increasing power swing by time. Simulation results agree Nyquist trajectory analysis well. Thus, in power sending system, PSS at first and fast excitation system (with small phase delay) as second are effective measure for improving oscillatory stability.

[**Power System Modeling**]   Demello's coefficients calculated of the five power system modeling as introduced before are shown in Table 6.4. Slow excitation system with PSS is adopted. Voltage sensitivity of reactive power is expressed by product of sensitivity itself βb and reactive power amount Qb. Demello's coefficient in transient condition are the same of those by CZ load.

Table 6.4 Load's voltage sensitivity and Demello's coefficients (send)

Agg. load		αb	βbQb	K_1	K_2	K_3	K_4	K_5	K_6
Y	IM	1.3527	-0.9678	0.0855	1.8442	0.7529	0.2970	-0.0725	1.7134
T	IM	1.0534	-0.3645	0.1360	0.9270	0.9232	0.2871	-0.0384	1.0851
Y	CI	1.2248	-0.6979	0.1116	1.3613	0.8189	0.2934	-0.0555	1.3924
T	CI	1.0217	-0.1494	0.1415	0.8238	0.9959	0.2833	-0.0336	0.9923
*	CZ	2	0.2503	0.1190	1.2266	1.7877	0.2424	-0.0299	0.9085

Damping torque coefficients are shown in Fig. 6.16. Three cases of traditional aggregation and CZ are stable. Two cases in Y-connection are unstable and especially IM load case is quite unstable.

Nyquist trajectories are shown in Fig. 6.17. In Y-connection cases stability is poor, and IM load case
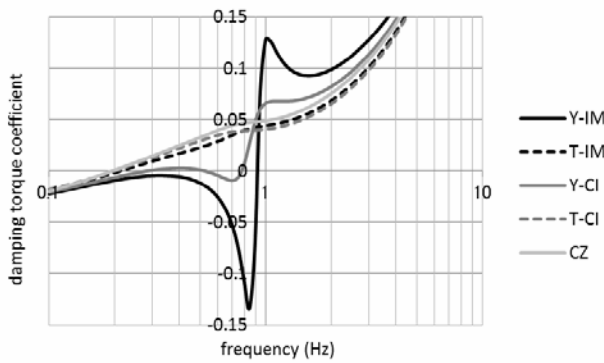
shows instability.

Fig. 6.16 damping torque by power system modeling (send)
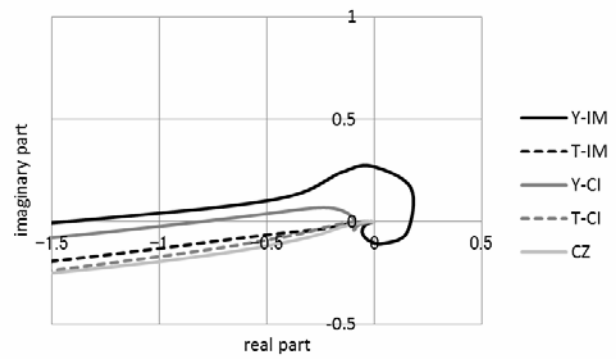

Fig. 6.17 Nyquist trajectory by power system modeling (send)
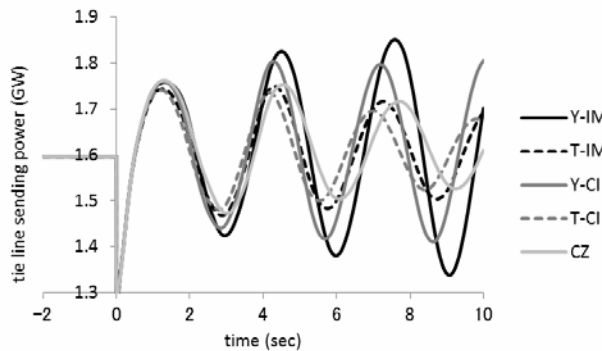

Fig. 6.18 Simulation result by power system modeling (send)

Simulation results by detailed power system model are shown in Fig. 6.18. Two Y-connection cases show poor stability. In addition, CI load cases show poorer stability than Nyquist trajectory analysis. Perhaps the difference was generated by aggregation error.

Thus as stated above, power system model that represents the truth faithfully by IM 50% load and Y-connection aggregation shows poor stability. On the contrary, the other modeling show quite optimistic results and they must be said as overlooking and misleading.

[RE Design]   Slow excitation system with PSS is assumed. Faithful power system model: IM 50% load and Y-connection aggregation is adopted.

Damping torque coefficients are shown in Fig. 6.19. Drop or FRT type RE case shows better stability than no RE case. DVS type RE case shows further better stability.
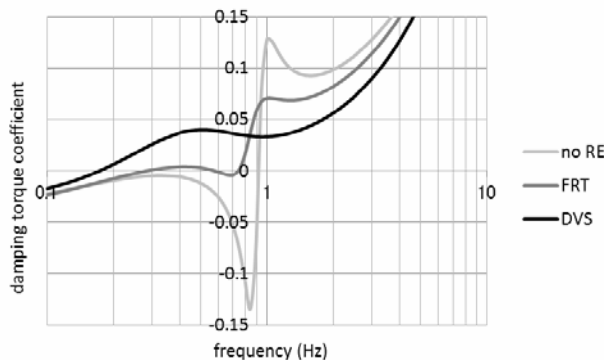

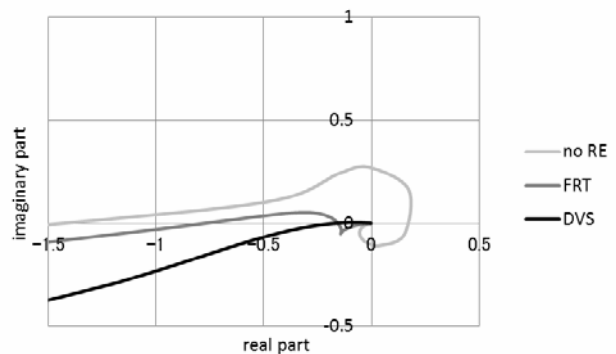Fig. 6.19 damping torque by RE design (send)

Fig. 6.20 Nyquist trajectory by RE design (send)

Nyquist trajectories are shown in Fig. 6.20. Drop or FRT type RE case is stable; while no RE case is

unstable. DVS type RE case is quite stable.

Simulation results are shown in 6.21. No RE case is unstable. Drop or FRT case that was stable in Nyquist trajectory analysis turns to slightly unstable. Perhaps the difference was brought by aggregation error. DVS RE case is quite stable.
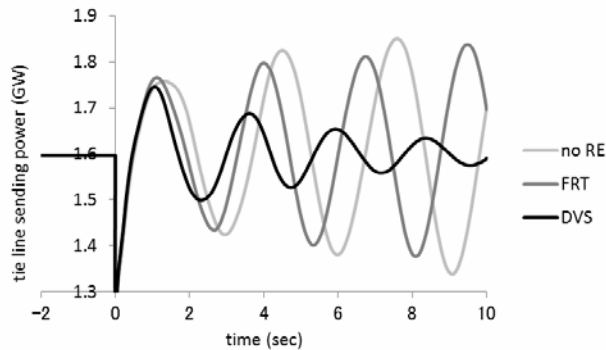

Fig. 6.21 Simulation result by RE design (send)

Thus in power sending power system, Drop or FRT type RE slightly improves oscillatory stability and DVS type RE improves very much.

Example of Power Receiving System

Structure of the example power receiving system is shown in Fig. 6.22. The system interconnects to outer system and receives much power via three tie lines. It is assumed that both 2 circuits of one tie line stop at F1 fault without any grounding. The system turns to a long and thin radial system receiving much power. Power flow conditions after fault are shown in Table 6.5.
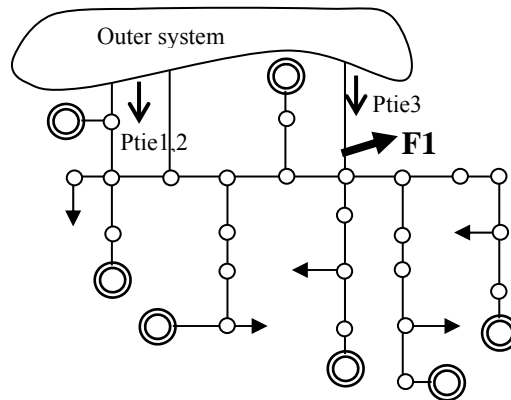

Fig. 6.22   Structure of the example receiving system

Table 6.5 Power flow condition of receiving system

Xt	Xs	Vt	Vb	Vs	Pg	Pb	Ps
0.1259	1.5990	1.02	1.0	1.0	0.8175	1.1021	-0.2846

[**IM Ratio**]   By varying IM ratio, Demello's coefficients in steady state vary as shown in Fig. 6.23. At a glance, a singular point exists at 70% IM ratio or a little smaller. At larger IM ratio K_2 turns to negative, which means that excitation increase results generator output decrease. In such a situation no excitation system can maintain stable operation.

106

All Demello's coefficients are positive at no IM. This is a special character of power receiving system, and means that oscillatory instability is less possible in power sending system.
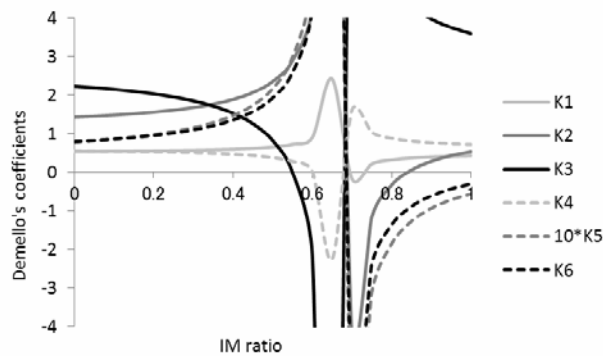

Fig. 6.23 Demello's coefficients by IM ratio (receive)

However as IM ratio increase, K_3 turns to negative at first and K_4 follows. That is, IM load brings oscillatory instability by negative K_3, and the instability is a different phenomenon from that by negative K_5 seen in power sending system. However, instability due to negative K_3 or K_4 can be mitigated by careful design of excitation system.

[Excitation System]   Four types of excitation system introduced above are compared. As system model, most realistic combination: IM 50% load and Y-connection aggregation is adopted. Damping torque coefficients are shown in Fig. 6.24. The value goes to negative at 1 Hz or faster frequency in case of slow excitation system. If PSS is used, negative region shifts to higher frequency but negative value survives. The negative value is not solved so long as slow excitation system is used.

Nyquist trajectories are shown in Fig. 6.25. In the figure, PSS that is believed as the best solution for oscillatory stability has negative effect. Fast excitation system shows good stability.
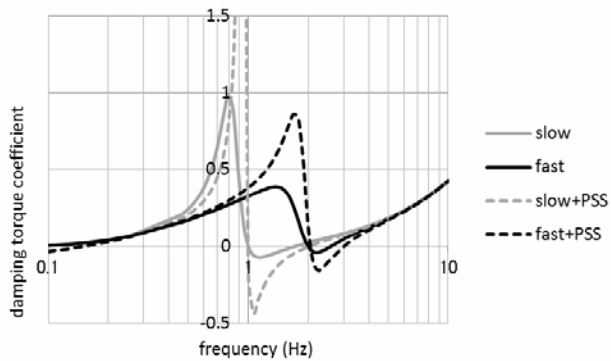

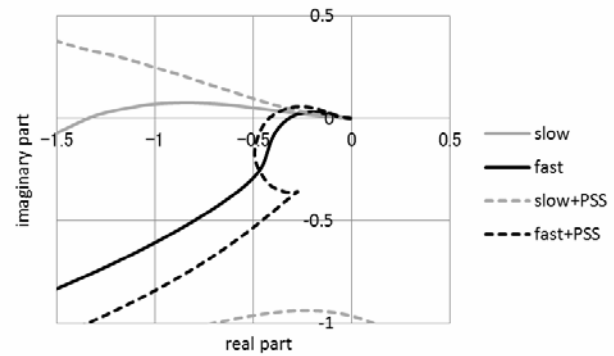Fig. 6.24 Damping torque by excitation system design (receive)   Fig. 6.25 Nyquist trajectory by excitation sys. design (receive)
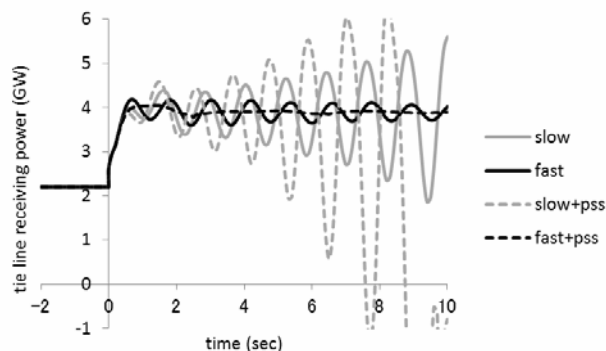

Fig. 6.26 Simulation result by excitation system design (receive)

107

Simulation results are shown in Fig. 6.26. In cases of slow excitation system, fast power swing with around 1 sec period becomes larger by time and PSS certainly shows negative effect. In cases of fast excitation system, the system turns to stable. However, result with PSS becomes worse than Nyquist trajectory analysis. Perhaps the difference was brought by aggregation error. In power receiving, fast excitation system is the first measure and PSS is the second measure, with contrast to sending system.

[Power System Modeling]   Load's voltage sensitivities seen from trunk bus and Demello's coefficients are calculated in the five power system modeling cases stated above. The results are shown in Table 6.6. Slow excitation system with PSS is adopted.

Table 6.6 Load's voltage sensitivities and Demello's coefficients (receive)

Agg.	load	αb	βbQb	K_1	K_2	K_3	K_4	K_5	K_6
Y	IM	1.4051	-0.9421	0.6561	2.3532	0.8239	0.3809	0.2168	1.9266
T	IM	1.0718	-0.2893	0.5602	1.0935	1.2792	0.5329	0.0979	0.9975
Y	CI	1.2488	-0.6288	0.5642	1.6159	0.9709	0.3990	0.1564	1.4330
T	CI	1.0319	-0.0768	0.5485	0.9938	1.3756	0.5440	0.0866	0.8986
*	CZ	2	0.2967	0.5495	1.4984	2.2261	0.5744	0.0834	0.8229

Damping torque coefficients are shown in Fig. 6.27. Three cases of traditional aggregation and CZ load show good stability. However, faithfully represented Y-connection cases show poor stabilities, and IM50% case shows ill stability.

Nyquist trajectories are shown in Fig. 6.28.   Similarly, Y-connection cases show poor stabilities, and IM 50% case shows ill stability.
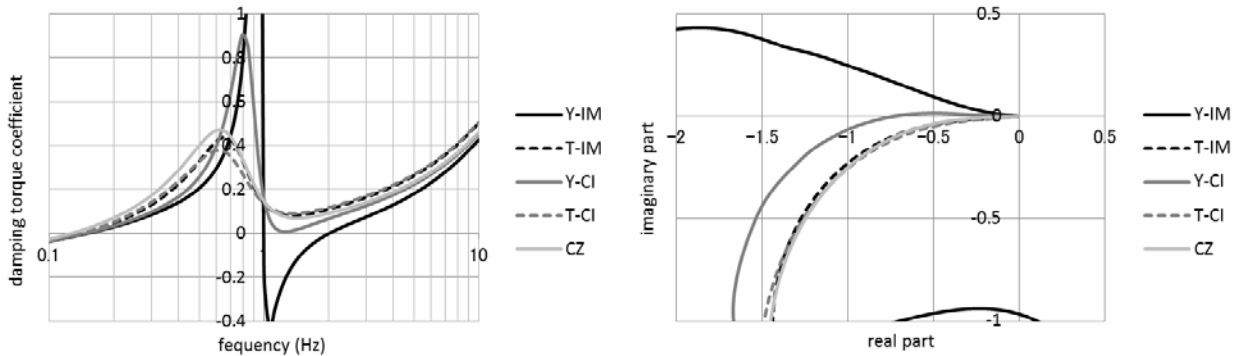

Fig. 6.27 Damping torque by power system modeling (receive)   Fig. 6.28 Nyquist trajectories by power sys. modeling (receive)
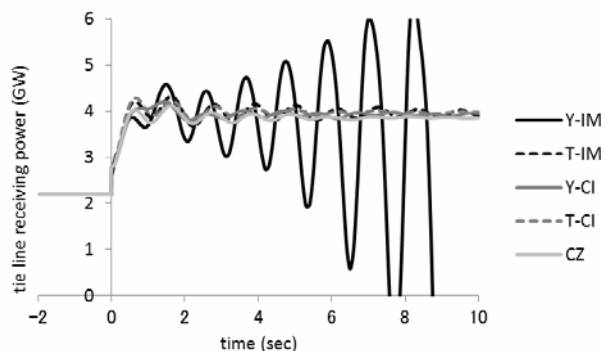

Fig. 6.29 Simulation results by power system modeling (receive)

Simulation results by detailed power system model are shown in 6.29. Y-connection cases show poor stabilities, and especially IM50% case shows quite ill stability. Simulation results agree Nyquist trajectory analysis well.

As stated above, comparing to faithfully represented IM50% load and Y-connection power system model, the other four power system models give optimistic assessments, and must be said as overlooking and misleading.

〔 **RE Design** 〕   Slow excitation system with PSS is assumed. IM50% load and Y-connection aggregation are adopted as faithfully represented power system model. Damping torque coefficients are shown in Fig. 6.30. FRT type RE case is unstable as well as no RE case. DVS type RE case is quite stable.

Nyquist trajectories are shown in Fig. 6.31. Similarly FRT type RE case is unstable as well as no RE case. DVS type RE case is quite stable.
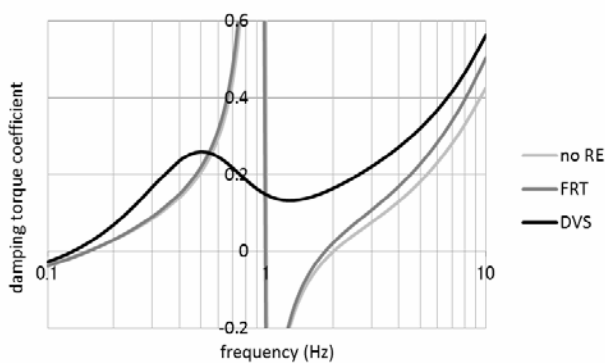

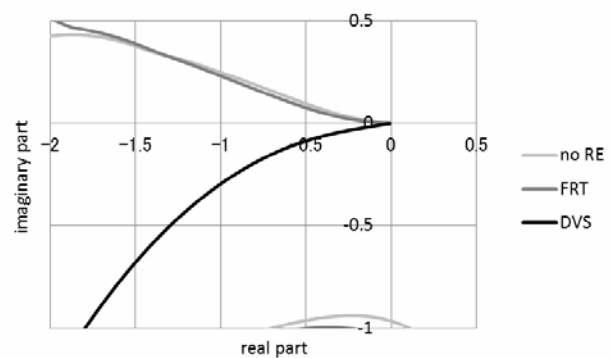Fig. 6.30 Damping torque by RE design (receive)   Fig. 6.31 Nyquist trajectories by RE design (receive)
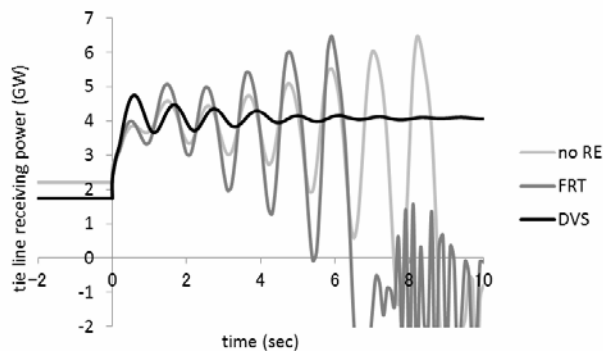

Fig. 6.32 Simulation results by RE design (receive)

Simulation results are shown in Fig. 6.32. FRT type RE case becomes worse than no RE case and worse than Nyquist analysis. Perhaps the difference is brought by aggregation error. DVS type RE case is quite stable.

As stated above, FRT type RE has no improving effect on oscillatory stability in power receiving system. On the contrary, DVS type RE has quite strong stabilizing effect also in receiving system.

The Deep Misunderstanding

It was at "Distribution Generators' Impact to Trunk System Investigation Working Group" settled in the "Central Electric Power Council" that oscillatory instability in power receiving system was introduced. IEEJ EAST30 and WEST30 power system model were modified by IM load and aggregation considering

network impedance to load terminal. By the modification power system became quite unstable and power swing very often appeared in not only power sending system but also receiving system. WG members said that the power system model was wrong, because such power swings never appeared in existing power system.

However, it was also a truth that excitation system employed in EAST30 and WEST30 model was very slow type and slower than slow excitation system used in the chapter. As the result, power swing became easily appear even in receiving system. Existing excitation system is much faster, so such power swing never appeared in existing system. Since such misunderstanding existed in the past, influence of excitation system on oscillatory stability is minutely studied both in sending and receiving system in the chapter.

Oscillatory stability is the physically and mathematically most difficult phenomenon to analyze among various stabilities. By the reason, there are very few engineers who analyze it using not simulation method. In addition, most of them are already retired. Because of the difficult analysis, successors are not grown up. The fact that one can analyze instability only by simulation means that he cannot understand instability mechanism and cannot propose countermeasures. The author wants to improve, however, "Wall of Fool" introduced by Dr. Yoro stands hardly.

References

(1) W. G. Heffron, R. A. Phillips: "Effect of a modern amplidyne voltage regulator on underexcited operation of large turbine generators", Trans. AIEE Vol. 71, Pt. β, Aug. 1952, pp.692-697

(2) Sekine: "Power system Analyses theories", Denki Shoin, 1971. (in Japanese)

(3) F. P. de Mello, C. Concordia: "Concepts of Synchronous Machines Stability as Affected by Excitation Control", IEEE Trans. PAS-88, Vol. 4, 316, 1969.

(4) S. Komami, T. Komukai, S. Kimura, and K. Koyanagi: "Effect of Load Characteristics on Dynamic Stability of Power System", IEEJ Trans. PE, Vol. 107, No. 7, pp. 341-348, 1987 (in Japanese, translated in English by Wiley)

(5) Komami: "Dynamic Stability of the System Receiving Power from Infinite Bus", IEEJ Annual Meeting PE, No. 30, 1990. (in Japanese)

(6) Y. Yamagishi & S. Komami: "Power System Dynamic Stability Analysis Considering Dynamic Load and Distributed Generation", IEEJ Trans. PE, Vol. 126, No. 10, pp. 977-984, 2006. (in Japanese)

(7) E. W. Kimbark, "Power System Stability Ⅲ Synchronous Machines", Wiley, 1956